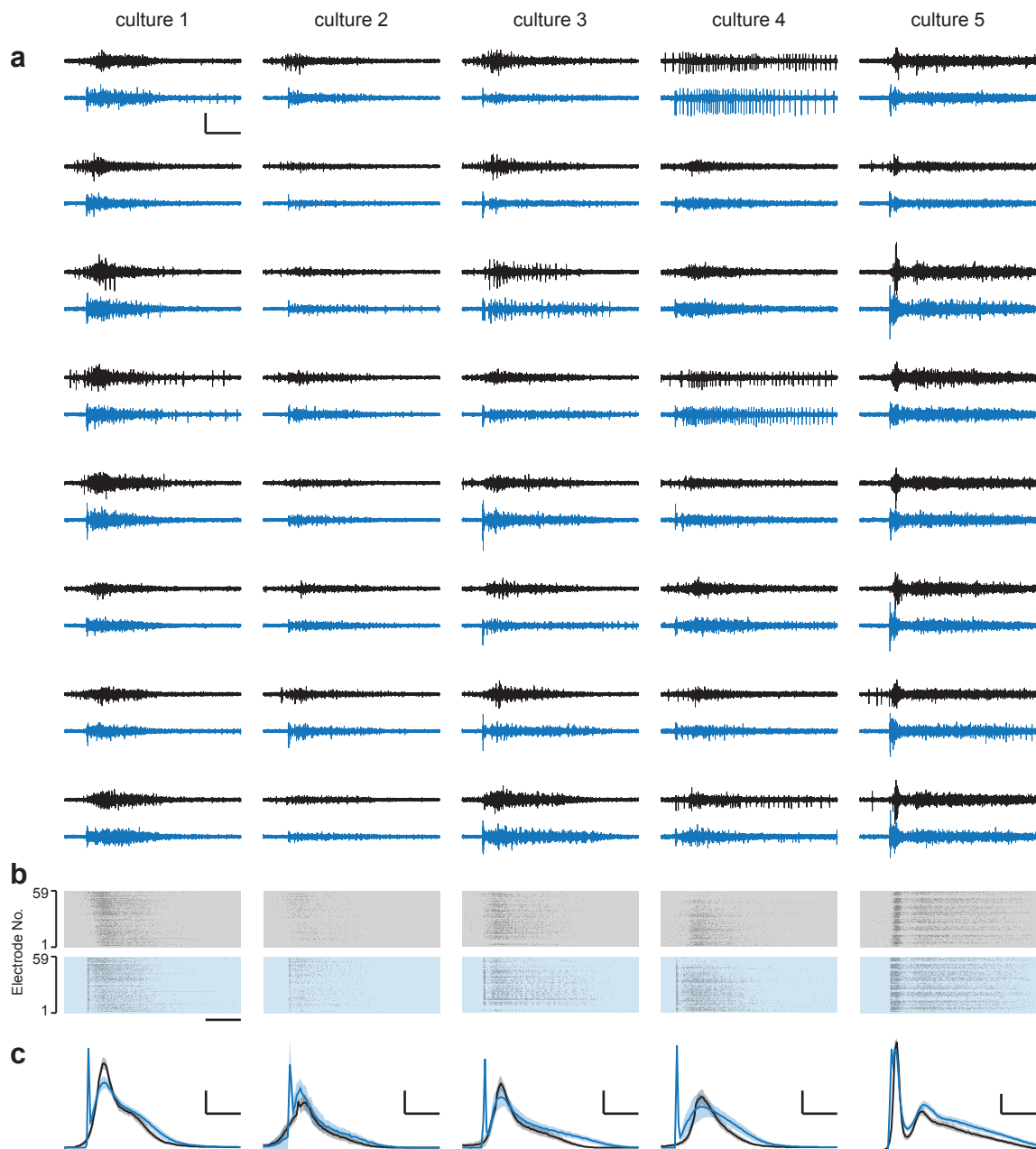


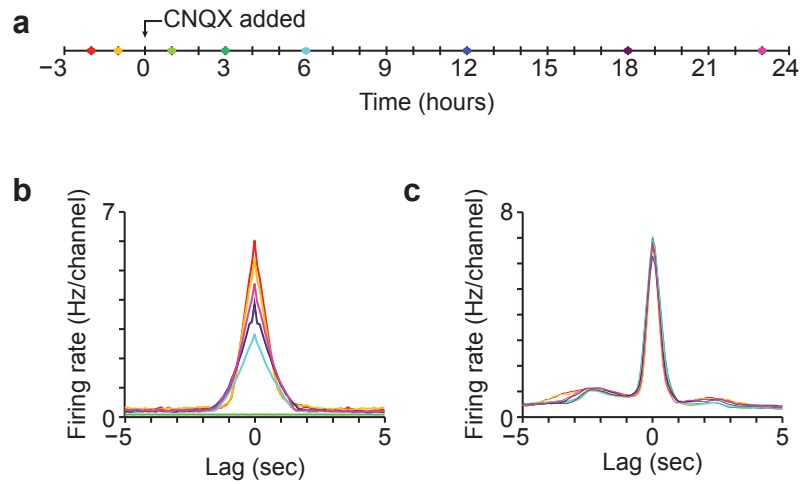
Supplementary Fig. 1: NMDAergic transmission is responsible for the late phase of bursts.

(a) *Left*, MEA-wide firing rate for culture treated with vehicle. Bin size, 1s. *Right*, average burst waveform before (black) and after (red) vehicle. Shading denotes s.d. Bin size, 10 ms. Scale bar, 1 kHz, 200 ms. (b, c) Same as (a) for CNQX- and APV-treated cultures. All recordings shown are from sister cultures were plated on a multi-well MEA, with each well containing 9 microelectrodes. When AMPAergic transmission is blocked, there is a slight delay in burst onset, but a pronounced increase in burst duration. When NMDAergic transmission is blocked, burst duration is significantly reduced. Together these suggest that AMPAergic transmission facilitates burst initiation and that NMDAergic transmission is responsible for burst elongation.

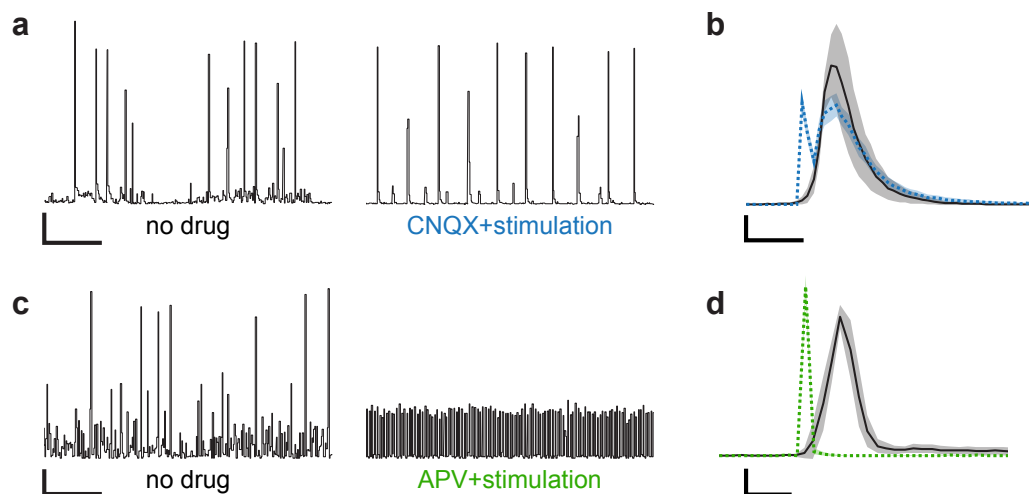
Supplementary Fig. 2: Frequency, Decay Kinetics, Charge for TTX/CNQX cultures (a) sflksjdf



Supplementary Fig. 3 : Optogenetic stimulation during CNQX treatment effectively mimics spontaneous bursts within individual cultures. (a) Raw voltage traces showing spiking activity on individual electrodes during a spontaneous burst in the absence of drugs (black), or a optically-evoked burst in the presence of CNQX (blue). Data is shown from all 5 chronically-photostimulated cultures, and the 8 electrodes that were most active during the pre-drug period were selected for display. Scale bars, 100 μ V, 200 ms. (b) Rastergrams showing spike times for all MEA electrodes corresponding to burst shown in (a). Grey background denotes spontaneous data, and blue background denotes condition with CNQX and optically-restored spiking. Scale bar, 200 ms. (c) Average MEA-wide firing rate during a burst (spontaneously-occurring, black, 6 hours of burst data; optically-evoked during CNQX, blue, 24 hours of burst data). Shaded regions denote s.d. Bin size, 10 ms. Scale bars, 5 kHz (cultures 1, 3, 4, 5), 2 kHz (culture 2), 200 ms (all).

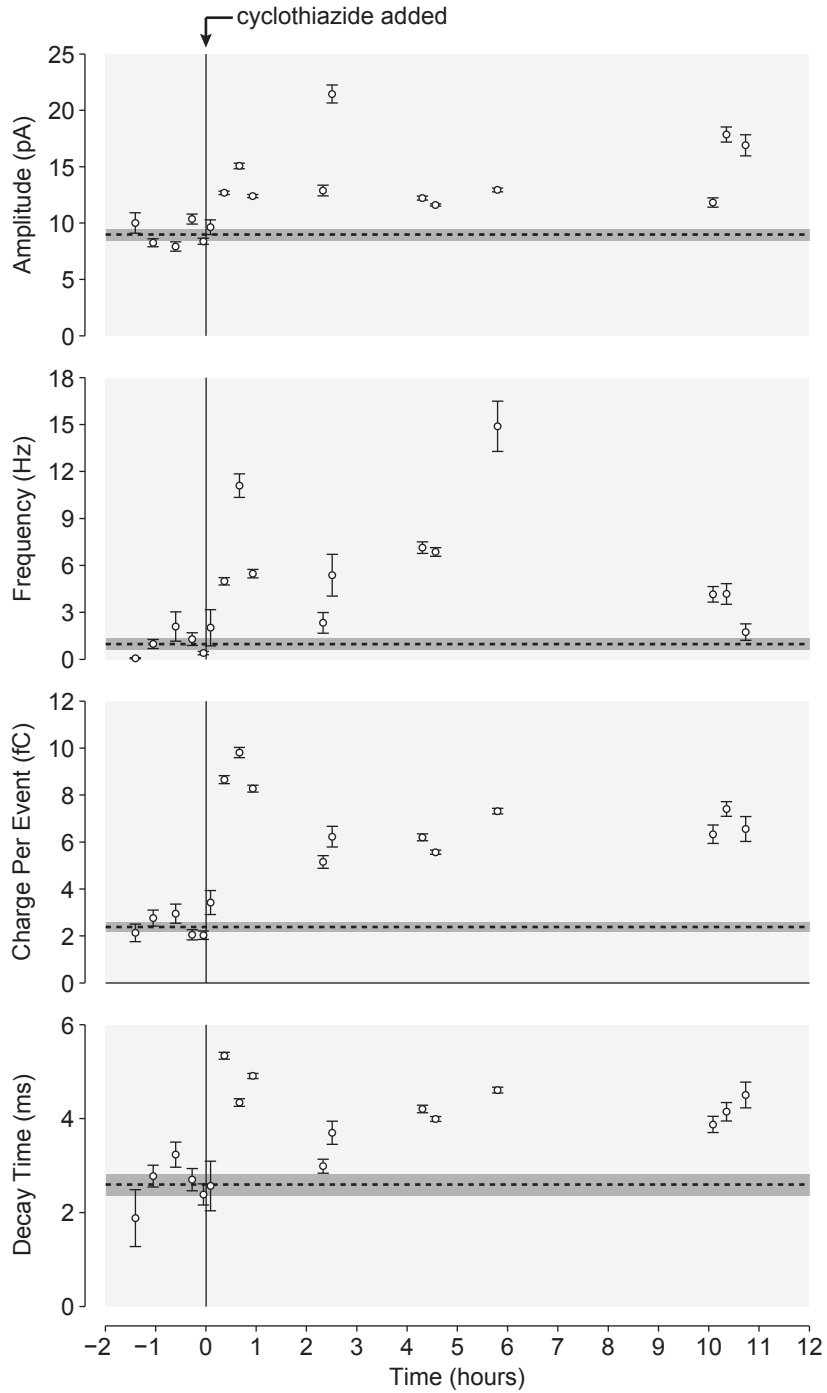


Supplementary Fig. 4: Optogenetic stimulation during CNQX treatment reproduces channel-to-channel correlations. (a) Timeline showing time points (colored dots) when channel-to-channel correlations were calculated. (b) Cross correlation function for CNQX-treated culture shown in Fig. 1d at different hours. Line colors correspond to dots in (a). (c) Cross correlation functions for culture shown in Fig. 3e, treated with CNQX and experiencing optogenetically-restored spiking levels. Stimulation restores pre-drug channel-channel correlations across the entire 24 hour treatment.

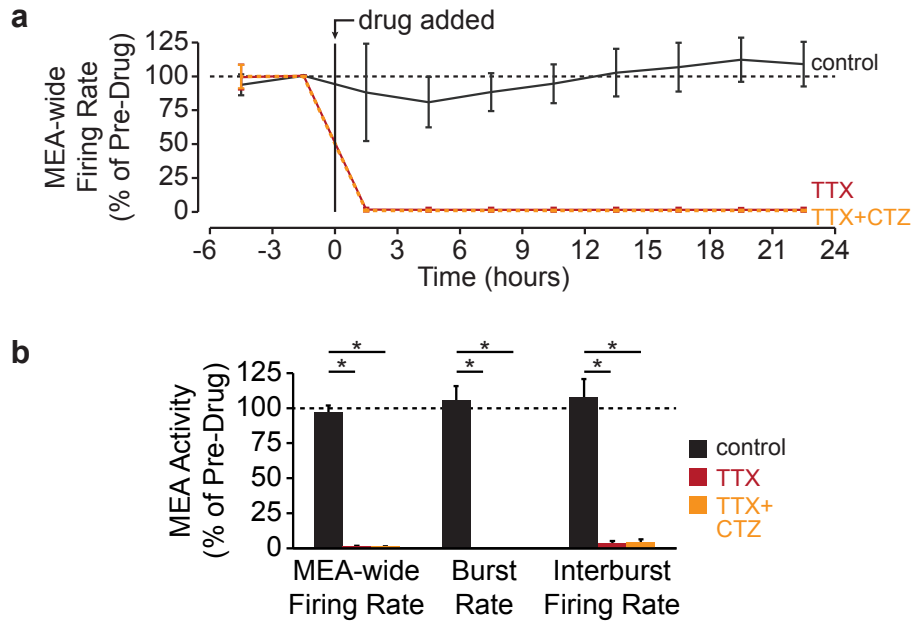


Supplementary Fig. 5: NMDAergic transmission facilitates normal bursting during optical stimulation. (a) MEA-wide firing rate for a culture (26 DIV) before drug treatment (left), and during CNQX treatment with optogenetically-restored firing rate (right). Bin size, 1s. Scale bars, 200 Hz, 1 min. (b) Average burst waveforms for the two conditions pre-drug (black) and CNQX+stimulation (blue) conditions. Data used to generate averages was taken for an hour before and after trace shown in (a). Bin size, 10 ms. Scale bar, 2 kHz, 100 ms. (c) MEA-wide firing rate for a culture (33 DIV) before drug treatment (left), and during APV treatment with optogenetically-restored firing rate (right). Bin size, 1s. Scale bars, 200 Hz, 1 min. (d) Average burst waveforms for the pre-drug (black) and APV+stimulation (green) conditions. Data used to generate averages was taken for an hour before and after trace shown in (c). Bin size, 10 ms. Scale bar, 800 Hz, 50 ms. Data shown in this figure was generated from cultures transfected with AAV2-CaMKIIa-ChR2(H134R)-mCherry, and recordings were performed at 26 DIV (a,b) and 31 DIV(c,d). All other plating, recording, and stimulation parameters were the same as other experiments previously described.

Supplementary Fig. 6: Frequency, Decay Kinetics, Charge for CNQX/CNQXstim1X cultures (a)
sdfkjsjdf



Supplementary Fig. 7: Cyclothiazide is effective at enhancing quantal AMPAR activation for at least 11 hours. mEPSCs were recorded from 4 different cells, using TTX and bicuculline to isolate AMPAergic events. CTZ was added and 11 additional cells over the course of 11 hours. Mean mEPSC amplitude, frequency, charge per event, and decay time is shown for all 15 cells. Point just before and after CTZ is added are the same cell. Dotted line denotes the pre-CTZ average of the 4 cell means. Shading and error bars denote s.e.m.



Supplementary Figure 8: Cyclothiazide does not change effects of TTX on spiking activity. (a) Mean MEA-wide firing rate over time for cultures treated with TTX+CTZ (n=5 cultures). Control and TTX values from Fig. 1e are shown for comparison. Bin size, 3h. Error bars denote s.d. (b) Mean MEA-wide firing rate, burst rate, and interburst firing rate for the cultures treated with vehicle, TTX, or TTX+CTZ during the 24-hour treatment window. TTX+CTZ completely abolished spiking and bursting (MEA-wide firing rate, $1.056 \pm 0.002\%$; burst rate, $0 \pm 0\%$; interburst firing rate, $4.26 \pm 1.91\%$, $p < xx$). Error bars denote s.e.m.

Supplementary Fig. 9: Frequency, Decay Kinetics, Charge for TTX/TTX+CTZ cultures (a)
sdfllksjdf